Effect of Added Block Copolymer on Phase-Separation Kinetics of a Polymer Blend. 1. A Light-Scattering Study

Ryong-Joon Roe* and Chung-Mien Kuo

Department of Materials Science and Engineering, University of Cincinnati, Cincinnati, Ohio 45221-0012

Received January 16, 1990; Revised Manuscript Received April 12, 1990

ABSTRACT: A light-scattering study has been made to investigate the effect of added styrene–butadiene diblock copolymer on the phase-separation kinetics of blends of low molecular weight polystyrene and polybutadiene. The scattered light intensity was measured at 2° intervals up to 60° as a function of time from the beginning of phase separation into the late stage of Ostwald ripening. Various corrections, including the one for double scattering, were applied to the observed intensity. The effect of the added block copolymer was to retard the growth of phase-separated domains, as seen from the time evolution of q_{max} and I_{max} of the peak in the intensity curve. This can be explained in terms of the reduction in the interfacial tension between the demixed phases, resulting from accumulation of block copolymer there. The time-evolution exponents of q_{max} and I_{max}, the invariant Q, and the superposition of scattering intensity curves all show the validity of dynamic scaling in the late ripening stage.

Introduction

One of the most important practical uses of block copolymers is as a compatibilizing agent[1] of polymer blends. There are numerous references in the literature attesting to the usefulness of block copolymers as compatibilizers. Electron micrographs[2-4] give the evidence that phase-separated domains in immiscible blends are rendered much smaller in dimension when block copolymer is added.

The word "compatibilization" in this context does not mean that immiscible polymer blends are rendered thermodynamically miscible by addition of block copolymer. In fact, our experimental results[5] with low molecular weight polystyrene–polybutadiene blends showed that while an added styrene–butadiene *random* copolymer depressed the cloud points significantly, an added styrene–butadiene *block* copolymer was incapable of producing a similar effect. Immiscible blends are rendered more translucent by addition of block copolymer because of the resulting reduction in the size of phase-separated domains. Improved mechanical properties of such blends also arise from a better adhesion between the phases due to the presence of block copolymer molecules at the interfaces.

The interfacial activity of block copolymer added to homopolymer blends has been investigated theoretically by Noolandi and Hong[6] and by Leibler[7] and was shown experimentally by interfacial tension measurement by Gaillard et al.[8] Preferential accumulation of the block copolymer molecules at the interface and consequent lowering of the interfacial tension between the two polymer phases are therefore considered to be the prime reason for the reduction in the phase-separated domain sizes.

Although the basic principle of the role played by block copolymer in blend compatibilization thus appears by now well established, clear understanding of the factors optimizing the efficacy of such compatibilization has not yet been attained. For example, no experimental data establishing the optimum amount of block copolymer or the optimum molecular weight for best performance have yet been published. In practical usage, moreover, the processing conditions of the polymer blend are such that thermodynamic equilibrium is usually not attained, and therefore considerations based on equilibrium aspects alone may not be sufficient. This provides us with a motivation to investigate the effect of added block copolymer on the phase-separation dynamics of homopolymer blends.

The phase-separation kinetics of polymer blends has been an active area of study by many in the last decade. Most of these studies focused on the early stages of spinodal decomposition[9-19] to compare the data against the predictions of linearized theories[20-23] of the spinodal decomposition process. Some of the studies were concerned also with the late stages[24,25] of the decomposition with a view, in particular, to ascertaining the applicability of the dynamic scaling concept. In this work, we are mainly interested in the very late stage of the phase separation, which is probably more important in determining the morphology of the blends in the final product than the early and intermediate stages of phase separation. We investigate the effect of added block copolymer in modifying the phase-separation dynamics. In this article, we report a light-scattering study of low molecular weight polystyrene–polybutadiene blend to which a small amount of styrene–butadiene block copolymer has been added. In a later article, we plan to report on the results of optical microscopic observation on similar blend systems.

Experimental Section

Materials. The polystyrene used was purchased from Pressure Chemical Co. and has $M_n = 1900$ and $M_w/M_n = 1.06$. The polybutadiene used was purchased from Goodyear Chemical Co. and has $M_n = 2650$ and $M_w/M_n = 1.13$. The styrene–butadiene diblock copolymer, kindly synthesized by Dr. H. L. Hsieh of Phillips Petroleum Co., has 52.5% styrene, $M_n = 25\,000$, and $M_w/M_n = 1.04$. This block copolymer is the same material used in previous studies.[5,26]

Light-Scattering Measurements. The light-scattering apparatus was designed and constructed in our laboratory. It consists of a low-power (2-mW) He–Ne laser, whose beam is sent vertically through a hole in a heating stage with a horizontal platform, on which a sample of a thickness of about 0.025 mm sandwiched between two cover glasses is placed. The scattered light intensity is measured by means of 30 photodiodes (EG&G HUV-1100BG) installed at 2° intervals to cover scattering angles 2–60°. Two additional photodiodes are installed, one to monitor the incident light beam intensity before entering the sample and the other to measure the transmitted beam. The outputs from the 32 photodiodes are fed into two 16-channel multiplexers (Metrabyte EXP-16), which are in turn connected to two channels of an analog-to-digital converter (Data Translation DT 2764-PGL) in a PDP 11/73 computer. The ADC board has a 12-bit resolution and a programmable gain of 1, 10, 100, or 500 times. A rapid, successive access to the photodiodes under a program control enables the reading of all 32 diodes in less than 0.2 s.

0024-9297/90/2223-4635$02.50/0

Scattered Intensity Corrections. The photodiode readings were first corrected for the dark current, the sensitivity of individual photodiodes relative to other diodes, and the fluctuation in the incident laser beam intensity. The scattering angle, θ (the angle between the incident beam and the scattered beam), within the sample is related to the observed scattering angle, θ_{obs}, by

$$n \sin \theta = \sin \theta_{obs} \quad (1)$$

where n is the refractive index of the sample (taken as 1.56 for all the blends studied). The moment transfer q is given by

$$q = 4\pi n \sin (\theta/2)/\lambda \quad (2)$$

where λ is the wavelength of the laser beam in vacuo (0.6328 μm). Because of the refraction at the sample–air interface, the constant solid angle in the air subtended by each photodiode corresponds to a solid angle within the sample that varies with θ. This refraction correction[27] is made by multiplying the observed intensity by

$$C_n = \frac{n^2 \cos \theta}{(1 - n^2 \sin^2 \theta)^{1/2}} \quad (3)$$

To correct for the loss of intensity due to scattering while the beam passes through the sample (turbidity correction) the observed intensity is also multiplied[27] by

$$\kappa = \frac{(-\ln T)(1/\cos \theta - 1)}{T - T^{1/\cos \theta}} \quad (4)$$

where T is the transmission of the sample (ratio of the transmitted to the incident beam intensity). Finally, a correction is applied to account for the fact that a part of the beam reaching the photodiodes has been scattered more than once within the sample. The method for correcting the effect of such multiple scattering is described in the Appendix. Even with the very thin samples employed, the transmission was reduced to 0.5 (or even below in some cases) at the very late stage of phase separation, and with such turbid systems the turbidity correction and the multiple-scattering correction were very important.

Results and Discussion

Blends having the following three compositions were studied: 80/20/0, 80/20/0.5, and 80/20/1, where the numbers refer to the relative amount (in weight) of polystyrene, polybutadiene, and styrene–butadiene block copolymer. Cloud points of these blends were found to be 114.0 ± 0.5, 113.0 ± 0.5, and 112.0 ± 0.5 °C, respectively. The addition of block copolymer is thus seen to lower the cloud point slightly. The blends exhibit an UCST behavior, and hence the phase separation was induced by a temperature jump from above the cloud point to 110 °C, which is below the cloud points of all the blends. The 80/20/0 blend was studied at 108 °C as well.

Figure 1 gives log–log plots of the intensity curves obtained with blend 80/20/0 at 110 °C at various times. (Note that successive intensity curves were multiplied by a factor $(10)^{1/2}$ to make the curves well separated vertically from each other for better legibility.) Scattering curves obtained at other temperatures and with other blends are qualitatively similar. The value of q_{max}, at which the intensity shows a maximum, shifts toward smaller q as the phase-separation progresses. Even at the very early stage, it is difficult to discern a time period during which q_{max} remains constant. In Figure 2, the logarithm of intensity is plotted against time for selected values of q. Evidently, exponential growth (or decay) of intensity with time is not realized at any q. In view of the rather shallow depth (4 °C) of quench below the cloud point, it is not certain whether the phase separation occurred by the spinodal decomposition mechanism. In any case, if there existed an early stage in which the linearized theory of spinodal decomposition was applicable, it must have passed very quickly even before our measurement began.

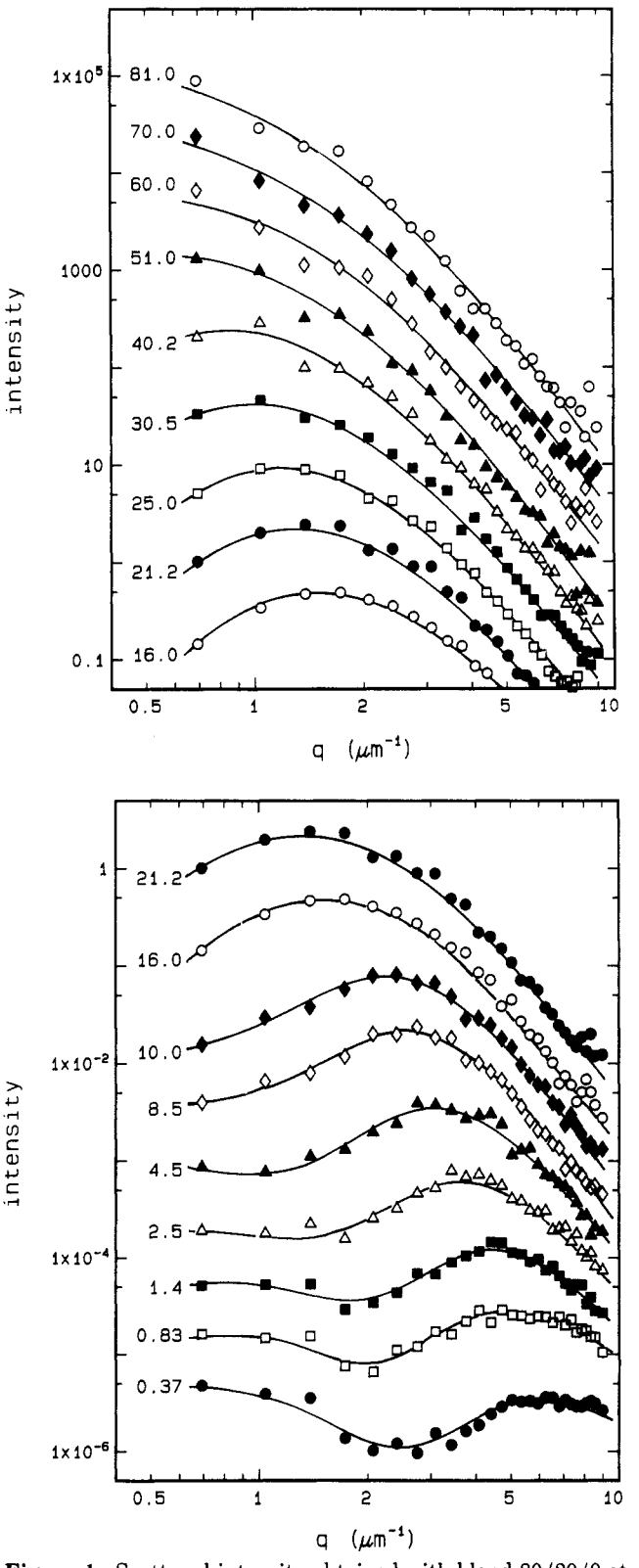

Figure 1. Scattered intensity obtained with blend 80/20/0 at 110 °C, after all the corrections described in the text have been applied, plotted against q. The time (in min) elapsed from the quench to 110 °C from above the cloud point is indicated on each curve. Successive curves have been shifted vertically by a factor of $(10)^{1/2}$ for legibility.

In Figure 3, q_{max} is shown against time in a log–log plot for all four runs. In Figure 4, the intensity maximum, I_{max}, is similarly plotted. The results for the two runs with the 80/20/0 blend at 108 and 110 °C superpose well with each other, showing that the difference in the supercooling between the two runs is not reflected on the growth rate of the phase-separated domains. The initial period of

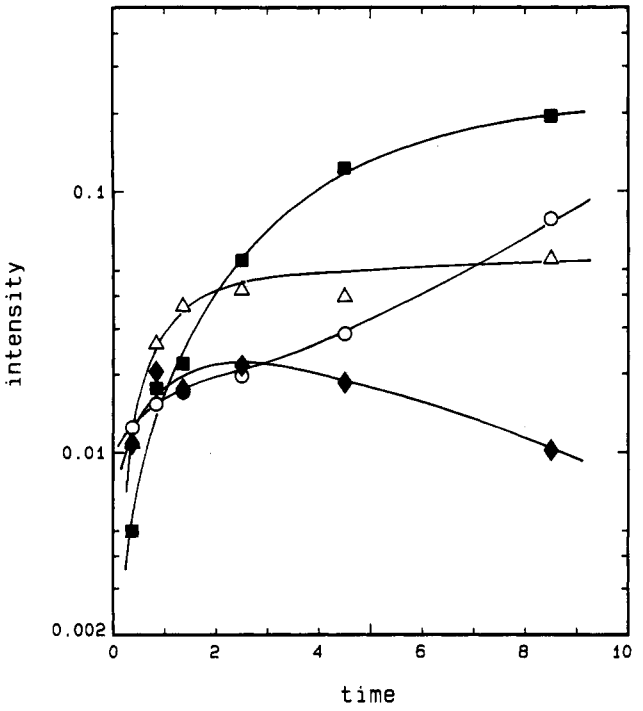

Figure 2. Intensity data given in Figure 1 plotted against time for selected q values: (○) q = 1.0, (■) q = 3.0, (△) q = 5.0, (♦) q = 7.0 μm^{-1}.

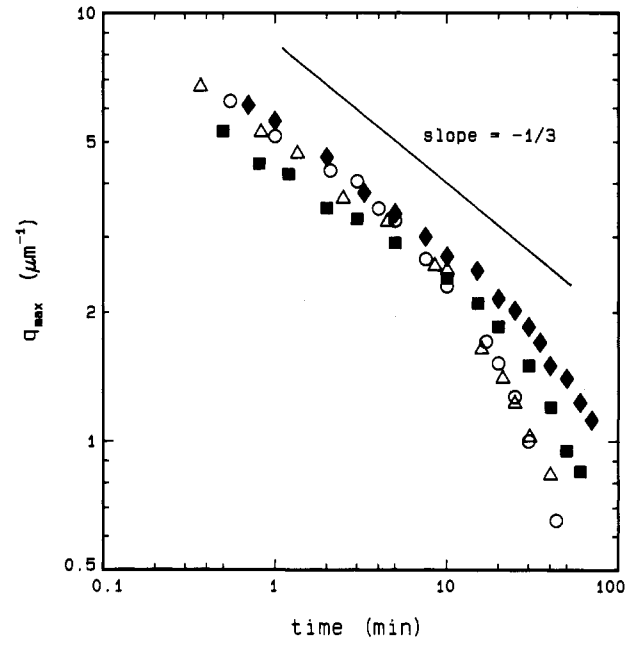

Figure 3. Value of q at the intensity maximum plotted against time: (○) 80/20/0 at 108 °C, (△) 80/20/0 at 110 °C, (■) 80/20/0.5 at 110 °C, (♦) 80/20/1 at 110 °C.

phase separation, either by spinodal decomposition or nucleation mechanism, is driven by the free energy difference between the homogeneous and phase-separated states and should, in general, be sensitively affected by the degree of supercooling below the coexistence curve. The insensitivity of the observed phase-separation process to the degree of supercooling reaffirms that the so-called early stage of the phase-separation process has been well completed by the time our measurement has even begun. In the later stage of the growth of phase-separated domains, the main thermodynamic factor determining the rate is now the absolute temperature rather than the degree of supercooling. Upon examination of the effect of added block copolymer, the phase-separation runs were therefore

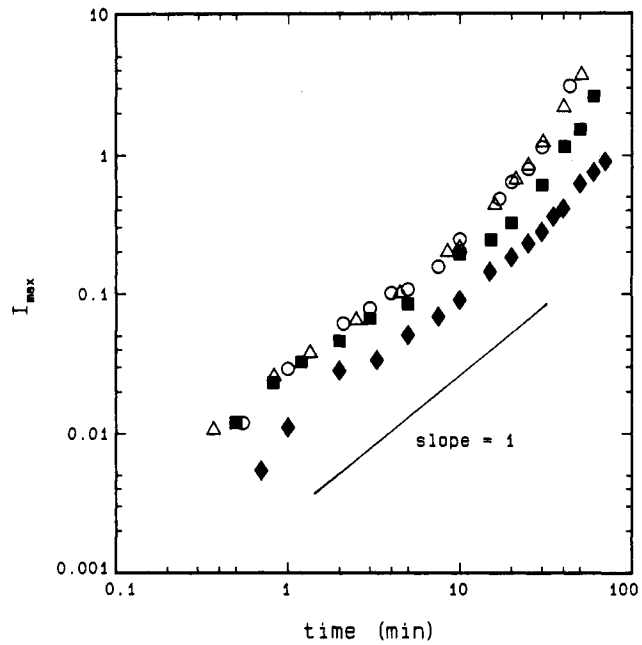

Figure 4. Intensity maximum plotted against time: (○) 80/20/0 at 108 °C, (△) 80/20/0 at 110 °C, (■) 80/20/0.5 at 110 °C, (♦) 80/20/1 at 110 °C.

made at the same temperature, 110 °C, rather than at the same degree of supercooling below the cloud points, which differ depending on the amount of block copolymer added.

Figures 3 and 4 show that the effect of added block copolymer is to retard the growth of phase-separated particles, and this tendency is recognizable more clearly at longer times in both figures. This finding can be explained as follows. When block copolymer is added to the system, the copolymer molecules tend to accumulate at the phase boundaries and thereby lower the interfacial tension.[6,7] The driving force for the particle ripening process, irrespective of whether it is by the evaporation–condensation[28] mechanism or by the coalescence mechanism, arises from the reduction in the free energy of the system realized when the total interfacial area is reduced by particle growth. The smaller the interfacial tension between the phases, the smaller is the reduction in the free energy for a given amount of reduction in the interfacial area. In the Lifshitz–Slyozov theory[28] of Ostwald ripening by the evaporation–condensation mechanism, the rate of growth of particle diameter is in fact expected to be directly proportional to the interfacial tension. In a separate study,[30] we are engaged in direct optical-microscopic observation of the growth of phase-separated particles in similar systems. The rate of growth of particle diameters determined by visual observations corroborates the conclusion, obtained from the light-scattering data in this study, that the main effect of added block copolymer is to retard the growth of phase-separated particles. The reduction in particle sizes in immiscible polymer blends realized by addition of block copolymers, as demonstrated directly by electron micrographs[2-4] or indirectly by improvement in mechanical properties,[1] has often been thought to imply that the added block copolymer prevents the particles from growing beyond a certain size dictated by the amount and characteristics of the block copolymer. The present results, however, suggest that the addition of block copolymer may have a significant effect mainly on the kinetic rather than on the equilibrium properties of the blends, and the reduced particle size frequently observed in the presence of block copolymer may arise not because the particle growth is arrested but rather because the particle growth is slower and their growth is therefore

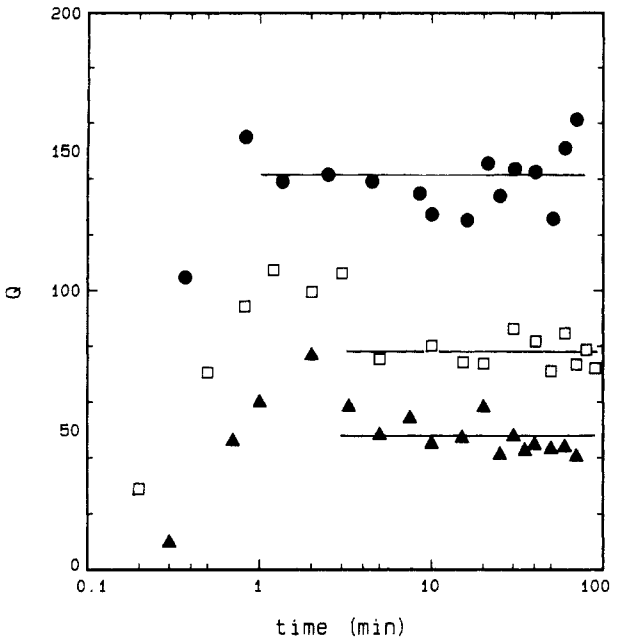

Figure 5. "Invariant" Q, evaluated according to eq 8, plotted against time: (●) 80/20/0, (□) 80/20/0.5, (▲) 80/20/1, all at 110 °C.

terminated more prematurely during the fixed time period available under given processing conditions.

In a power law expression of the time evolution of q_{max}, the exponent ϕ in

$$q_{max} \propto t^{\phi} \tag{5}$$

is seen in Figure 3 to be approximately equal to $-1/3$ in most of the time except toward the end of the time period studied. Similarly, the exponent θ in

$$I_{max} \propto t^{\theta} \tag{6}$$

is seen in Figure 4 to be approximately equal to 1 in the comparable time period. Hence

$$\theta/\phi = -3 \tag{7}$$

Relation 7 appears to hold even toward the end of the time period studied, when a decrease in ϕ below $-1/3$ is accompanied by an increase in θ above 1. Relation 7 is expected to hold in general[31] in the late stage of phase separation when the compositions within the demixed phases and the relative amounts of the two phases no longer change with time. Another indication to the same effect can be obtained by evaluating the so-called "invariant" Q by

$$Q = 4\pi \int_0^{\infty} q^2 I(q)\, dq \tag{8}$$

The values of Q obtained by numerical integration of the observed scattered intensity, $I(q)$, are shown in Figure 5. For a two-phase system with sharp interfacial boundaries, Q is related[32] to

$$Q = (2\pi)^3 V\phi(1-\phi)(\Delta n)^2 \tag{9}$$

where V is the scattering volume, ϕ is the volume fraction of one of the phases, and Δn is the refractive index difference between the two phases. Although there is considerable scatter in the data points in Figure 5, one can still discern that the values of Q remain unchanged beyond about 3 min of the phase separation, suggesting that the values of ϕ and Δn remain constant during the rest of the phase-separation process. The relative magnitudes of Q in the three blends are also in line with the expectation

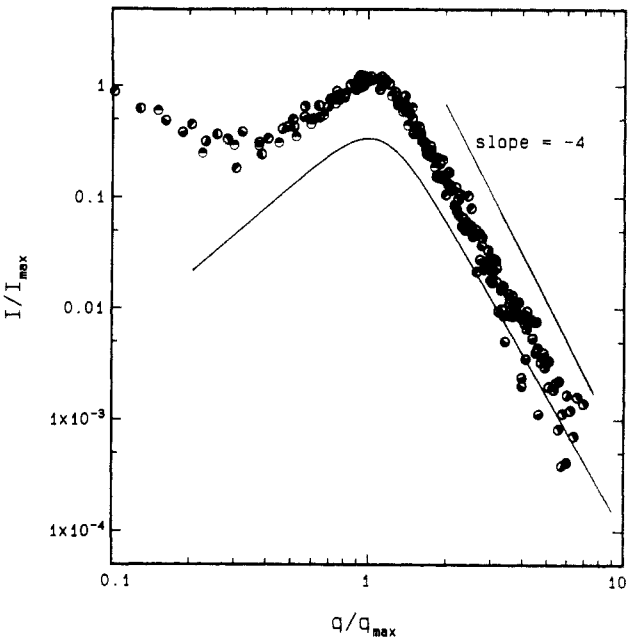

Figure 6. Intensity curves obtained with 80/20/1 at 110 °C, at different times, except those at 2 min or shorter, plotted to show the superposition obtainable when I/I_{max} is plotted against q/q_{max}. The solid line is the theoretical curve calculated by eq 10 (and shifted downward by a factor of 3 for legibility).

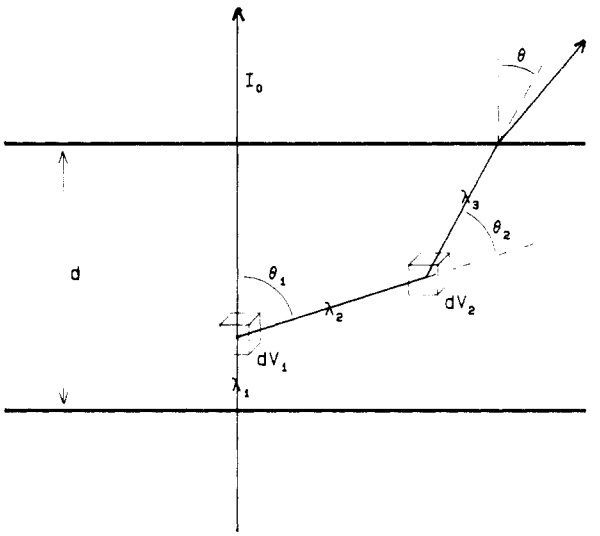

Figure 7. Schematic diagram illustrating the geometry of a doubly scattered beam. The incident beam, I_0, is scattered at dV_1 by angle θ_1 and is scattered again at dV_2 by angle θ_2, to emerge from the sample at the overall scattering angle θ. The path length of the beam through the sample is $\lambda_1 + \lambda_2 + \lambda_3$.

that the volume fraction, ϕ, of the minority phase decreases as the cloud point is reduced from 114 to 113 and to 112 °C with increasing block copolymer concentration.

The results shown in Figures 3–5 suggest that the changing patterns of light scattering observed in this work arise as the result of the changes in the particle sizes of the minority phase, which has attained its final, equilibrium composition already in the very early stage, perhaps within 1–2 min after the temperature jump to below the cloud point. Under this condition, the particle size distribution is likely to retain a self-similarity with time, which permits analysis of the data by application of the dynamic scaling concept. That this indeed is the case is demonstrated in Figure 6, where I/I_{max} is plotted against q/q_{max} with the data obtained with blend 80/20/1 at different t for $t > 2$ min. (Only half of the available data points have been plotted in Figure 6 to avoid excessive overlapping.) All

the curves are seen to superpose on top of each other into a single curve, except for very small values of q/q_{max} at which an anomalous upturn in the scattered intensity is observed. According to the theoretical analysis by Furukawa,[33] the scaled structure function is given by

$$I/I_{max} = \frac{3(q/q_{max})^2}{2 + (q/q_{max})^6} \tag{10}$$

A curve calculated according to eq 10 is also plotted in Figure 6 for comparison. (The calculated curve has been shifted downward by a factor of 3 for the sake of legibility.) The agreement is fairly satisfactory, although at q/q_{max} values greater than 1 the experimental curve attains the asymptotic slope of −4 sooner than the calculated curve. The asymptote

$$I_{max} \propto (q/q_{max})^{-4} \tag{11}$$

which eq 10 reduces to for large values of q/q_{max}, is known as Porod's law[32] in the analysis of small-angle X-ray scattering data. The good accord of the data to Porod's law indicates that our blend sample studied contains a two-phase system with boundaries that are sharp in comparison to the wavelength of light.

Acknowledgment. This work has been supported in part by the U.S. Army Research Office and also by the donors of the Petroleum Research Fund, administered by the American Chemical Society.

Appendix. Correction for Double Scattering

Theoretical expressions relating the scattered light intensity function, $I(\theta)$, to the structure of the sample usually assume that the incident rays are scattered only once in the sample before it exits the sample surface. However, when the scattering power of the sample is high in comparison to the sample size, an appreciable fraction of the scattered rays undergoes an additional scattering before they leave the sample. Given below is the procedure we utilized to correct for such double scattering. The extent of triple or higher order scattering is much smaller and is assumed negligible in this work.

The problem of multiple scattering has been examined mostly in connection with X-ray scattering.[33-36] The expressions derived in these studies are applicable to the present case with only a minor modification to the notations.

In the absence of multiple scattering, the intensity $I_1(\theta)$ of light scattered in the direction θ is given by

$$I_1(\theta) = I_0 \frac{1}{r^2} R'(\theta)\, P_1(\theta)\, V e^{-\tau\lambda} \tag{A1}$$

where I_0 is the incident light intensity, r is the distance between the sample and the detector, V is the scattering volume, τ is the turbidity, λ is the pass length of the light through the sample, $R'(\theta)$ is the Rayleigh ratio and $P_1(\theta)$ is the (single-scattering) polarization factor. Note that the Rayleigh ratio, $R(\theta)$, as customarily defined includes the polarization factor, $P_1(\theta)$. For the present purpose it is, however, more convenient to separate $P_1(\theta)$ from the Rayleigh ratio $R'(\theta)$, so that $R(\theta) = R'(\theta)\, P_1(\theta)$. $P_1(\theta)$ is given by

$$P_1(\theta) = {}^1/_2(1 + \cos^2\theta) \tag{A2}$$

in the case of unpolarized incident light but takes a different expression when it is polarized. The turbidity, τ, is the measure of the light intensity lost due to scattering when the ray traverses a unit distance within the sample. The loss of the light energy due to absorption is here considered to be negligible. The turbidity is then related to $R'(\theta)$ by

$$\tau = 2\pi \int_0^\pi R'(\theta)\, P_1(\theta) \sin\theta\, d\theta \tag{A3}$$

In the geometry of our light-scattering instrument, the incident ray enters the sample at a right angle to the surface. Consider a ray scattered at first at the volume element dV_1 and then scattered again at dV_2 before reaching the opposite surface at a net scattering angle θ (see Figure 7). The total distance the ray has traversed within the sample is $\lambda_1 + \lambda_2 + \lambda_3$, and the angles of scattering at dV_1 and dV_2 are θ_1 and θ_2, respectively. Note that the ray between dV_1 and dV_2 does not necessarily lie in the plane defined by the incident and exitant rays, although it is not made clear in the two-dimensional diagram of Figure 7. The intensity of light $dI_1(\theta_1)$ reaching dV_2 after a single scattering at dV_1 is given by

$$dI_1(\theta_1) = I_0 \frac{1}{\lambda_2^2} R'(\theta_1)\, P_1(\theta_1) \exp[-\tau(\lambda_1 + \lambda_2)]\, dV_1 \tag{A4}$$

After the secondary scattering at dV_2, the intensity $dV_2(\theta)$ of the ray emerging from the surface is

$$dI_2(\theta) = I_0 \frac{R'(\theta_1)}{\lambda_2^2} \frac{R'(\theta_2)}{r^2} P_2(\theta_1,\theta_2,\theta) \times \exp[-\tau(\lambda_1 + \lambda_2 + \lambda_3)]\, dV_1\, dV_2 \tag{A5}$$

The intensity of the ray emerging in the direction θ as a result of double scattering is then given by integration of $dI_2(\theta)$ over all the possible locations of both dV_1 and dV_2 throughout the irradiated sample volume

$$I_2(\theta) = \int dI_2(\theta) \tag{A6}$$

while the corresponding single-scattering intensity is given by

$$I_1(\theta) = \int dI_1(\theta) \tag{A7}$$

To apply the double-scattering correction, the observed intensity has to be multiplied by $I_1(\theta)/[I_1(\theta) + I_2(\theta)]$.

The polarization factor, $P_2(\theta_1,\theta_2,\theta)$, for double scattering, in the case of an unpolarized incident beam, is given by

$$P_2(\theta_1,\theta_2,\theta) = {}^1/_2[(\cos^2\theta_1 + \cos^2\theta_2) + (\cos\theta - \cos\theta_1 \cos\theta_2)^2] \tag{A8}$$

For a polarized incident beam, the expressions for P_1 and P_2 can be found in the paper by Strong and Kaplow.[35]

Since the volume element dV_1 can be located anywhere along the incident beam direction within the thickness of the sample and the volume element dV_2 can be anywhere within the sample, the integral expressed in eq A6 is in fact a quadrupole integration. A special computational trick such as a Monte Carlo sampling[35] was resorted to in the past, but in this work the integration was performed readily on a PDP 11/73 when a moderately large grid size for the integration was used. At first, the observed intensity, scaled to the absolute intensity scale by means of eq A3, was used as a first approximation to $R'(\theta)$. The magnitude of corrections was fairly large. In the case where the transmission T was about 0.5, the ratio of I_2/I_1 was approximately 30%. In general, the result of the application of the correction was to accentuate the peaks and valleys in the $I(\theta)$ curve, much as one would find after correction for any type of instrument broadening.

References and Notes

(1) Paul, D. R. In *Polymer Blends*; Paul, D. R., Newman, S., Eds.; Academic Press: New York, 1978; Vol. 2, Chapter 12.
(2) Inoue, T.; Shoen, T.; Hashimoto, T.; Kawai, H. *Macromolecules* **1970**, *3*, 87.
(3) Fayt, R.; Jerome, R.; Teyssie, Ph. *J. Polym. Sci., Polym. Lett. Ed.* **1981**, *19*, 79; *J. Polym. Sci., Polym. Phys. Ed.* **1981**, *19*, 1269; 1982, *20*, 2209.
(4) Fayt, R.; Hadjiandreou, P.; Teyssie, Ph. *J. Polym. Sci., Polym. Chem. Ed.* **1985**, *23*, 337.
(5) Rigby, D.; Lin, J. L.; Roe, R. J. *Macromolecules* **1985**, *18*, 2269.
(6) Noolandi, J.; Hong, K. M. *Macromolecules* **1982**, *15*, 482; **1984**, *17*, 1531.
(7) Leibler, L. *Makromol. Chem., Macromol. Symp.* **1988**, *16*, 1.
(8) Gaillard, P.; Ossenbach-Sauter, M.; Riess, G. *Makromol. Chem. Rapid Commun.* **1980**, *1*, 771.
(9) Van Aartsen, J. J.; Smolders, C. A. *Eur. Polym. J.* **1970**, *6*, 1105.
(10) Snyder, H. L.; Meakin, P.; Reich, S. *Macromolecules* **1983**, *16*, 641.
(11) Nojima, S.; Tsutsumi, K.; Nose, T. *Polym. J.* **1982**, *14*, 225.
(12) Nojima, S.; Ohyama, Y.; Yamaguchi, M.; Nose, T. *Polym. J.* **1982**, *14*, 907.
(13) Kuwahara, N.; Tachikawa, M.; Hamano, K.; Kenmochi, Y. *Phys. Rev.* **1982**, *A25*, 3449.
(14) Hamano, K.; Tachikawa, M.; Kenmochi, Y.; Kuwahara, N. *Phys. Lett.* **1982**, *90A*, 425.
(15) Hashimoto, T.; Kumaki, J.; Kawai, H. *Macromolecules* **1983**, *16*, 641.
(16) Izumitani, T.; Hashimoto, T. *J. Chem. Phys.* **1985**, *83*, 3694.
(17) Strobl, G. R. *Macromolecules* **1985**, *18*, 558.
(18) Han, C. C.; Okada, M.; Muroga, Y.; McCrackin, F. L.; Bauer, B. J.; Tran-Cong, Q. *Polym. Eng. Sci.* **1986**, *26*, 3.
(19) Hill, R. G.; Tomlins, P. E.; Higgins, J. S. *Polymer* **1985**, *26*, 1708.
(20) Cahn, J. W. *Acta Metall.* **1961**, *9*, 795; *J. Chem. Phys.* **1965**, *42*, 93.
(21) de Gennes, P.-G. *J. Chem. Phys.* **1980**, *72*, 4756.
(22) Pincus, P. *J. Chem. Phys.* **1981**, *75*, 1996.
(23) Binder, K. *J. Chem. Phys.* **1983**, *79*, 6387.
(24) Hashimoto, T.; Itakura, M.; Hasegawa, H. *J. Chem. Phys.* **1986**, *85*, 6118.
(25) Takahashi, M.; Horiuchi, H.; Kinoshita, S.; Ohyama, Y.; Nose, T. *J. Phys. Soc. Jpn.* **1986**, *55*, 2687.
(26) Rigby, D.; Roe, R. J. *Macromolecules* **1986**, *19*, 721.
(27) Stein, R. S.; Keane, J. J. *J. Polym. Sci.* **1955**, *17*, 21.
(28) Lifshitz, I. M.; Slyozov, V. V. *J. Phys. Chem. Solids* **1961**, *19*, 35.
(29) Siggia, E. D. *Phys. Rev.* **1979**, *A20*, 595.
(30) Park, D. W.; Roe, R. J., to be submitted for publication.
(31) Nose, T. *Phase Transitions* **1987**, *8*, 245.
(32) Porod, G. *Kolloid Z.* **1951**, *124*, 83.
(33) Furukawa, H. *Physica* **1984**, *123A*, 497.
(34) Warren, B. E.; Mozzi, R. L. *Acta Crystallogr.* **1966**, *21*, 459.
(35) Strong, S. L.; Kaplow, R. *Acta Crystallogr.* **1967**, *23*, 38.
(36) Wignall, G. D.; Jarvis, J. A. J.; Munsil, W. E.; Pings, C. J. *J. Appl. Crystallogr.* **1974**, *7*, 366.
(37) Dwiggins, C. W., Jr.; Park, D. A. *Acta Crystallogr.* **1971**, *A27*, 264.
(38) Dwiggins, C. W., Jr. *Acta Crystallogr.* **1972**, *A28*, 155.

Registry No. Polystyrene, 9003-53-6; polybutadiene, 9003-17-2; (styrene)(butadiene) (block copolymer), 106107-54-4.